

The liquid-vapour interface of the restricted primitive model (RPM) of ionic fluids

This article has been downloaded from IOPscience. Please scroll down to see the full text article.

2000 J. Phys.: Condens. Matter 12 2637

(<http://iopscience.iop.org/0953-8984/12/12/306>)

View [the table of contents for this issue](#), or go to the [journal homepage](#) for more

Download details:

IP Address: 171.66.16.218

The article was downloaded on 15/05/2010 at 20:32

Please note that [terms and conditions apply](#).

The liquid–vapour interface of the restricted primitive model (RPM) of ionic fluids

Volker C Weiss[†] and Wolfram Schröer

Institut für Anorganische und Physikalische Chemie, Universität Bremen, D-28359 Bremen, Germany

Received 21 September 1999

Abstract. The liquid–vapour interface of the restricted primitive model (RPM) of ionic fluids is investigated within a square-gradient theory. We compute density profiles and interfacial tensions for different temperatures using Debye–Hückel (DH) theory and its recent extension for ion-pair formation and interactions between the dipolar ion pairs and free ions developed by Fisher and Levin. This Fisher–Levin (FL) theory is known to give an accurate description of the coexistence curve of the RPM. To account for the inhomogeneities in the interfacial region, the local free-energy density is expanded in terms of the density gradient. For small gradients, e.g. reasonably close to the critical point, such an expansion can be truncated after the square-gradient term. The coefficient of the latter is calculated from the direct correlation function using an approximate (quadratic) hypernetted-chain (AHNC) relation and, alternatively, from an extended van der Waals approach in conjunction with different approximations to the local density. The results from the AHNC relation and various local density approximations in the thermodynamic framework of DH theory and FL theory, respectively, are compared, and it is asserted that the AHNC relation in conjunction with FL theory predicts reliably the interfacial properties of the RPM even within this simple square-gradient theory. In contrast to the situation for simple fluids, the local density approximation must be chosen carefully for ionic fluids since properties such as the interfacial thickness and the surface tension may vary by a factor of three or four depending on the applied local density approximation.

1. Introduction

The properties of electrolytes, or ionic fluids in general, have aroused renewed interest in the context of an apparently classical (mean-field-like) critical behaviour of these fluids, which was suspected to be caused by long-range Coulombic interactions. About a decade ago, Singh and Pitzer [1] published the liquid–liquid coexistence curve of the salt tri-ethyl-*n*-hexyl ammonium tri-ethyl-*n*-hexyl borate dissolved in diphenyl ether, which could be described by the classical exponent of $\beta = 1/2$. Subsequent measurements of the turbidity of this system by Zhang *et al* [2] yielding the exponent $\gamma = 1$ seemed to support the view that this, indeed, was a classical system. (Later experiments by Wiegand *et al* [3], in which only Ising-type behaviour was found, have cast serious doubts on these earlier measurements.) For other systems, solutions of the organic salt tetra-*n*-butyl ammonium picrate in long-chain alcohols of low dielectric permittivity, Narayanan and Pitzer [4] observed asymptotic Ising-type behaviour, but in sharp contrast to what is found for simple fluids and fluid mixtures, a crossover from regular behaviour away from the critical point to the asymptotic Ising-like behaviour occurred only very close to the critical point, i.e. at unusually low reduced temperatures.

[†] Present address: Department of Chemistry, Baker Laboratory, Cornell University, Ithaca, NY 14853-1301, USA.

Motivated by the astonishing experimental findings reported in [1] and [2], several groups set out to explain the observed effects theoretically. Most theoretical studies of electrolytes are based on the simplest model of ionic fluids, the restricted primitive model (RPM). Within this model, the ionic fluid consists of charged hard spheres of equal diameter σ , half of which carry a charge of $+q$, the other half a charge of $-q$. These spheres are immersed in a dielectric continuum of dielectric constant ϵ . Reduced thermodynamic variables, temperature and number density, appropriate to this model are introduced via $T^* = kT\epsilon\sigma/q^2$ and $\rho^* = \rho\sigma^3$, where k is Boltzmann's constant.

The first step in the theoretical investigations was to find or develop a theory which predicts the location of the critical point and the coexistence curve correctly. From Monte Carlo simulations of the RPM, the critical point was known to be located somewhere in the region $T^* = 0.05$ – 0.06 and $\rho^* = 0.025$ – 0.05 [5–7]. Thus, it was concluded that the existing 'standard' theories for ionic fluids, the Debye–Hückel (DH) theory ($T_c^* = 0.0625$, $\rho_c^* = 0.005$), the mean-spherical approximation (MSA, $T_c^* = 0.0786$, $\rho_c^* = 0.0145$) and its self-consistent version, the generalized (G)MSA ($T_c^* = 0.0785$, $\rho_c^* = 0.015$) do not suffice to account for the thermodynamic behaviour of the RPM [8, 9]. Since both of these major types of theories underestimate the critical density, there were attempts to include the effect of ion pairing, which is known to be pronounced near the critical point [10, 11] and which, at a given total density, reduces the density of free ions. This in turn means that the overall ionic density needed to produce a particular density of free ions, which apparently governs the phase transition (at least within DH-based theories), is increased. Pairing theories based on the MSA were put forward by Stell and co-workers [12], who included interactions between dipolar ion pairs and free ions, and by Guillot and Guissani [13], who also accounted for dipole–dipole interactions. All theories rooted in the MSA, however, tend to yield too high a critical temperature ($T_c^* > 0.07$), even though the critical density was successfully increased. The DH-based theories must be viewed as more successful with regard to predicting the critical temperature. Levin and Fisher [14] allowed for Bjerrum ion pairing and accounted for the dipole–ion interaction by solving the linearized Poisson–Boltzmann equation as is done in DH theory for ion–ion interactions. This Fisher–Levin (FL) theory predicts a coexistence curve in substantial agreement with simulation results; furthermore the critical point parameters are $T_c^* = 0.05740671$ and $\rho_c^* = 0.02775$, reasonably close to the results of the simulations of Caillol [6] and of Orkoulas and Panagiotopoulos [7]. To our knowledge, there have been two attempts to improve upon FL theory by accounting for dipole–dipole interactions. Guillot and Guissani [13] just added the dipole–dipole term from the usual Onsager theory for dipolar fluids, while the present authors developed a more consistent fusion of DH theory and the Onsager model [15]. Both approaches, however, lead to lower critical densities as compared to FL theory and thus yield coexistence curves in worse agreement with simulations. At the moment, the FL theory must be regarded as the most successful theory for the RPM. More recent simulations, applied in conjunction with finite-size scaling techniques [16, 17] and, thereby, accounting for critical fluctuations, estimate the critical point to be at $T_c^* = 0.049$ and $\rho_c^* = 0.07$ – 0.08 , which is at higher densities and lower temperature than the earlier predictions. The fact that the FL theory as a mean-field theory overestimates the critical temperature (and, due to the pronounced asymmetry of the coexistence curve, underestimates ρ_c^*) is not surprising. Note, however, that the revised location of the critical point still lies on the diameter of the FL coexistence curve. Despite the shift in the critical parameters following from the more recent simulations, the location of the coexistence curve away from the critical point is unchanged, so the good agreement with the results of FL theory remains valid [17]. For our purpose here, the study of interfacial properties, which are evaluated at 'safe' distances from the critical point, the FL theory is reliable.

Having now at hand more or less accurate theories for the thermodynamic bulk properties of the RPM, the question of the crossover scale is addressed by applying the Ginzburg criterion. The so-called Ginzburg temperature signals the breakdown of a mean-field description as the critical temperature is approached on the critical isochore. Thus, the Ginzburg criterion estimates the extent of the critical region and provides the crossover scale [18].

All that is needed to apply the Ginzburg criterion in addition to a thermodynamic theory which predicts a critical point is the square-gradient term in the Landau–Ginzburg expansion of the free-energy density. This term can be obtained from the direct correlation function C_{ik} . Within the MSA, the direct correlation function is given by $C_{ik}(r > \sigma) = -\beta u_{ik}$, where $\beta = 1/kT$ and u_{ik} denotes the interaction potential between two particles. For the RPM, this pairwise interaction potential is given by $u_{ik} = q_i q_k / \epsilon r_{ik}$, where r_{ik} denotes the distance between particles i and k . Due to the electroneutrality condition, this contribution vanishes entirely, so the MSA predicts an unphysical, negative coefficient of the square-gradient term, which is caused by the hard-sphere part. Because of this pathological feature of the MSA, the first application of the Ginzburg criterion to the RPM by Leote de Carvalho and Evans employed the GMSA, which, because of the additional terms in the direct correlation function that ensure thermodynamic self-consistency, yields a positive coefficient of the square-gradient term [19]. The second approach, by Lee and Fisher [20], used the FL theory and functional differentiation to obtain the direct correlation functions and the square-gradient term from a DH equation which was generalized to inhomogeneous systems. This generalized (G)DH theory also yields the correct expression for the correlation length in the low-density limit, as was shown later by Bekiranov and Fisher by evaluating the cluster integrals explicitly [21]. GDH theory predicts the correlation length to diverge as $\xi = (b/9216\pi\rho)^{1/4}$ in the low-density limit, where $b = \sigma/T^*$ is the Bjerrum length. The third attempt to calculate the Ginzburg temperature of ionic fluids was also based on the DH theory and its extensions, but employed the approximate (quadratic) hypernetted-chain (AHNC) relation $C_{ik} = -\beta u_{ik} + (1/2)h_{ik}^2$ to relate the known pair correlation functions, the total pair correlation function h_{ik} or, equivalently, the pair distribution function g_{ik} , to the direct correlation function [22]. Alternatively, different local density approximations were applied to calculate the square-gradient term from the theory for the homogeneous system by an extended van der Waals *ansatz* [22]. All three approaches briefly outlined above agree that the Ginzburg temperature of the RPM should not be smaller than that of a simple fluid with short-range interactions. So, the experimental findings of mean-field-type criticality or unusually small regions of nonclassical Ising-like behaviour cannot be explained or rationalized by a Ginzburg-type analysis.

In our calculations using the extended van der Waals approach [22], the coefficient of the square-gradient term turned out to be extremely sensitive to the local density approximation that was applied to calculate it from the pair distribution function of the homogeneous system. This sensitivity causes a variation of the Ginzburg temperature over four orders of magnitude [23]. It became clear that such a sensitivity, which is not observed for simple fluids [22, 24], would affect all quantities that may be calculated from a square-gradient theory, such as interfacial properties, although to a lesser extent than the Ginzburg temperature, because the coefficient of the square-gradient term, c , enters the expression for the surface tension with a power of $1/2$ (see section 2.2 below), which is to be contrasted with the third power in the Ginzburg temperature. Discrepancies between the Ginzburg temperatures within the various local density approximations of three or four orders of magnitude will, thus, correspond to factors of three or even almost five by which the predicted surface tensions differ. Since the coefficient of the square-gradient term also enters the Ornstein–Zernike correlation length ξ as $c^{1/2}$ and the interfacial thickness is approximately given by $4\xi_l$, where ξ_l is the correlation length in the liquid phase, we can expect similar factors to appear in these properties as well.

The unusually strong dependence of the square-gradient term (and all properties that can be calculated from it) for the ionic fluid within DH theory came as a surprise since, for simple fluids, this dependence is known to be rather weak [22,24]. We attribute this peculiarity of ionic fluids to their exceptional virial expansion: the thermodynamic behaviour of simple fluids, like e.g. a square-well fluid with a reasonably short-range interaction potential, is dominated by the second virial coefficient [22] (in addition to the ideal-gas part). The partial pair distribution function corresponding to the second virial coefficient, however, is just the Boltzmann factor of the pair potential, $\exp(-\beta u_{ik})$, and is, therefore, density independent. This, in turn, implies that the local density approximation employed to calculate the square-gradient term is irrelevant on the level of the second virial coefficient. Differences stemming from the applied local density approximations enter through the third and higher virial coefficients, whose contributions are minor in the region where a square-gradient theory is expected to be valid, i.e. at comparatively low densities and, therefore, small density gradients [22]. For ionic fluids, however, the second virial coefficient does not represent the major contribution in any sense: the first term to describe deviations from the ideal behaviour—given by the Debye–Hückel limiting law—is of order $\rho^{3/2}$ and, thus, of lower order than the second virial coefficient. Furthermore, the pair distribution function corresponding to this term does depend on the density through the Debye screening length. Therefore the local density approximations affect the square-gradient term even at very low densities. At higher densities, there will be contributions from the limiting law as well as from higher (ionic) virial coefficients that keep the second virial coefficient from playing a dominating role comparable to that in the situation for simple fluids.

Recently, Groh *et al* calculated the interfacial tension and density profiles for the liquid–vapour interface of the RPM using the MSA [25]. Since the MSA direct correlation function yields, as mentioned above, no reasonable results for the square-gradient term, they obtained a ‘constructed’ direct correlation function from the pair correlation function h_{ik} by means of a local density approximation, namely the LADA (‘locally averaged density approximation’), which assumes the relevant density at which to evaluate the correlation function to be given by $\bar{\rho} = (\rho(r) + \rho(r'))/2$. This enabled them to obtain properties of the inhomogeneous fluid even though using the direct correlation function of the MSA (without further approximations) would have yielded nothing of value at this point.

As a direct consequence of the experience gained in the computations of the Ginzburg temperature, we calculated the density profiles and surface tensions for the liquid–vapour interface of the RPM within DH theory using different local density approximations to compute the square-gradient term within a gradient theory [23]. As suspected from the large differences of the Ginzburg temperatures in the various local density approximations, the surface tension as well as the interfacial thickness vary by a factor of three depending on which local density approximation is employed because of the above-mentioned square-root dependence of these quantities on the coefficient of the square-gradient term. The only criterion that can be used to decide which value is to be believed is the behaviour of the correlation length in the low-density limit. The GDH theory of Lee and Fisher and the AHNC relation yield the exact result, while the LADA treatment leads to a wrong prefactor of $\sqrt{14}$ in front of the correct Lee–Fisher expression. This prefactor pertains, almost unchanged, to finite densities—that is, to the correlation length in the liquid phase ξ_l , to the interfacial thickness, which is approximately given by $4\xi_l$, and to the interfacial tension as well [23] (cf. table 1). Thus one might suspect (although this has not been proved since the MSA may behave in a different way to the DH theory for different local density approximations) that a similar factor may be present in the results of Groh *et al*, and in the discussion section of this paper we will give an argument in support of this proposition.

Even though the DH-based treatment [23] demonstrated the relevance of the local density approximation to the interfacial properties, one cannot expect to obtain numerically reliable results for the interfacial properties of the RPM from it, as the description of the thermodynamic behaviour of this system by DH theory is rather poor [14] (see also figure 1). It is the purpose of this paper to calculate the interfacial properties within the much more accurate FL theory using reliable methods to obtain the square-gradient term in a gradient theory. After an outline of the theory employed in section 2, we briefly review the results for the DH-based calculation, which already appeared in this journal in a letter to the editor [23], and compare them to the predictions within FL theory in section 3. This section will also contain a discussion of the results obtained and an attempt to clarify the relation to the approach of Groh *et al*, which goes beyond the square-gradient theory. Section 4 summarizes the main conclusions of this work.

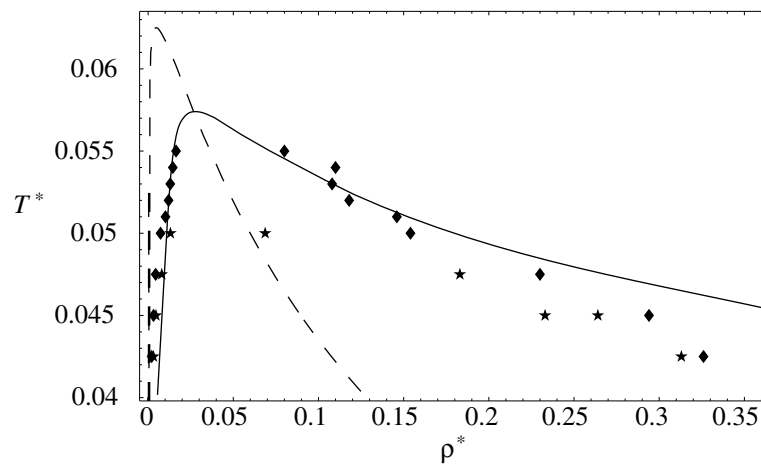


Figure 1. Coexistence curves for the Debye–Hückel theory (dashed) and for the Fisher–Levin theory (continuous), and simulation results of Caillol [6] (diamonds) and of Orkoulas and Panagiotopoulos [7] (stars).

2. Methodology

The computation of interfacial properties, like e.g. the interfacial tension, calls for an evaluation of the free-energy density of nonuniform systems. In principle, this evaluation would require the correlation functions appropriate to the inhomogeneous fluid; as these are basically unknown, one usually relies on approximation schemes, which allow for an approximate treatment based on the correlation functions of homogeneous fluids. One of these methods is the gradient theory, in which the local free energy is expanded in powers of the density gradient to account for the contribution of inhomogeneities. For small gradients, this expansion may be truncated after the square-gradient term. In this square-gradient theory (which is also called Landau–Ginzburg theory in a different context, but here the concept goes back to van der Waals), the local free-energy density consists of two terms: the free energy of a corresponding homogeneous system plus the square-gradient term that arises from inhomogeneities. The main advantage of this approach is that *both* terms can be calculated from the correlation functions of uniform fluids, either from the pair distribution function g_{ik} or from the direct correlation function C_{ik} . This procedure will be outlined in the following. In a second subsection, we will briefly summarize how the interfacial properties are calculated within the square-gradient

theory. The third subsection contains the details of the application of the formalism to the RPM within DH and FL theory.

2.1. Square-gradient theory

As mentioned in the introduction to this section, the free energy of a nonuniform system can be determined in principle. This total free energy consists of three terms: $A = A^{\text{id}} + A^{\text{hc}} + A^{\text{res}}$. The ideal-gas part A^{id} is known and the hard-sphere contribution A^{hc} will play no role in the present study because of the low densities involved. The residual part can be obtained from

$$\beta A^{\text{res}} = \frac{1}{2} \int_0^\beta \int \int \sum_{i,k} \rho_i(\mathbf{r}) \rho_k(\mathbf{r}') u_{ik}(r_{ik}) g_{ik}(\mathbf{r}, \mathbf{r}', \beta; \{\rho\}) d\mathbf{r} d\mathbf{r}' d\beta \quad (1)$$

where $\beta = 1/kT$, ρ_i is the number density of species i at \mathbf{r} , u_{ik} is the interaction potential between particles of species i and k , while g_{ik} is the pair distribution function for the nonuniform system. As such it depends not only on the separation r_{ik} , but explicitly on both loci \mathbf{r} and \mathbf{r}' as well as on the set of all densities (abbreviated by $\{\rho\}$) and their spatial distribution. Unfortunately, these pair distribution functions for the inhomogeneous system are unknown. To make any progress, one may, as an extension of van der Waals' theory of surface tension, replace the functional $g_{ik}(\mathbf{r}, \mathbf{r}', \beta; \{\rho\})$ by the function $g_{ik}(\mathbf{r}, \mathbf{r}', \beta, \rho_1(\mathbf{r}_m), \dots, \rho_n(\mathbf{r}_m))$ [22]. The densities ρ_p with $p = 1, \dots, n$ are supposed to include all relevant species, whose densities enter with their value at an as yet unspecified, but fixed position \mathbf{r}_m somewhere on the line connecting \mathbf{r} and \mathbf{r}' . As it is not clear *a priori* which point \mathbf{r}_m on that line is to be chosen, we set $\mathbf{r}_m = \mathbf{r} + z\mathbf{r}_{ik}$, with $\mathbf{r}_{ik} = \mathbf{r}' - \mathbf{r}$, so that z takes on values between 0 and 1. Then we expand the residual part of the local free-energy density of species i , $\phi_i(\mathbf{r}) = \beta A_i(\mathbf{r})\sigma^3/V$, given by

$$\begin{aligned} \phi_i^{\text{res}}(\rho_i(\mathbf{r}), \beta, \rho_1(\mathbf{r}_m), \dots, \rho_n(\mathbf{r}_m)) \\ = \frac{\sigma^3}{2} \rho_i(\mathbf{r}) \sum_k \int_0^\beta \int \rho_k(\mathbf{r}') u_{ik}(r_{ik}) g_{ik}(\mathbf{r}, \mathbf{r}', \beta, \rho_1(\mathbf{r}_m), \dots, \rho_n(\mathbf{r}_m)) d\mathbf{r}' d\beta \end{aligned} \quad (2)$$

where V is the volume, in terms of \mathbf{r}_{ik} , about \mathbf{r} . After truncation at the square-gradient level and an integration by parts, which converts terms of the type $\rho_i(\mathbf{r}) \nabla^2 \rho_k(\mathbf{r})$ into $\nabla \rho_i(\mathbf{r}) \cdot \nabla \rho_k(\mathbf{r})$, one is left with the two contributions that arise in the square-gradient theory:

$$\phi_{i,\text{hom}}^{\text{res}}(\mathbf{r}) = \frac{\sigma^3}{2} \rho_i(\mathbf{r}) \sum_k \rho_k(\mathbf{r}) \int_0^\beta \int u_{ik}(r_{ik}) g_{ik}(r_{ik}, \beta, \rho_1(\mathbf{r}), \dots, \rho_n(\mathbf{r})) d\mathbf{r}_{ik} d\beta \quad (3)$$

$$\begin{aligned} \phi_{i,\nabla^2}^{\text{res}}(\mathbf{r}) = & -\frac{\sigma^3}{12} \nabla \rho_i(\mathbf{r}) \cdot \sum_k \nabla \rho_k(\mathbf{r}) \int_0^\beta \int r_{ik}^2 u_{ik}(r_{ik}) \\ & \times g_{ik}(r_{ik}, \beta, \rho_1(\mathbf{r}), \dots, \rho_n(\mathbf{r})) d\mathbf{r}_{ik} d\beta \\ & - \frac{\sigma^3}{12} \sum_k \sum_{p=1}^n [z^2 \rho_k(\mathbf{r}) \nabla \rho_i(\mathbf{r}) + (1-z)^2 \rho_i(\mathbf{r}) \nabla \rho_k(\mathbf{r})] \cdot \nabla \rho_p(\mathbf{r}) \\ & \times \int_0^\beta \int r_{ik}^2 u_{ik}(r_{ik}) \frac{\partial g_{ik}(r_{ik}, \beta, \rho_1(\mathbf{r}), \dots, \rho_n(\mathbf{r}))}{\partial \rho_p(\mathbf{r})} d\mathbf{r}_{ik} d\beta. \end{aligned} \quad (4)$$

Equation (3) represents the free-energy density of a hypothetical homogeneous system with the set of densities $\{\rho(\mathbf{r})\}$, while (4) gives the square-gradient contribution to the local free-energy density.

To obtain explicit numerical results for a particular model fluid, we need to fix the value of z . This is equivalent to selecting a relevant density (at \mathbf{r}_m) at which to evaluate the pair distribution functions. At this point, the local density approximations come into play. The simplest, naive treatment would be to take no account of the local density and to evaluate the pair distribution functions at the mean overall density (MODA [23]). In a more elaborate (and more reasonable) approach, one may regard the density at a position halfway between \mathbf{r} and \mathbf{r}' as the relevant one and approximate $\bar{\rho} = \rho((\mathbf{r} + \mathbf{r}')/2)$ (‘density at average position approximation’, DAPA). Equally reasonable is to average the densities at the two loci and set $\bar{\rho} = (\rho(\mathbf{r}) + \rho(\mathbf{r}'))/2$ (‘locally averaged density approximation’, LADA). A fourth approach [22,23] averages over all values of z (‘Boltzmann-averaged position approximation’, BAPA, since, ideally, the contribution of each value of z would be weighted by the Boltzmann factor that this particular value of z produces in the free energy). If the averaging is performed with equal weights, one obtains $\langle z^2 \rangle = \langle (1 - z)^2 \rangle = 1/3$. As seen in (4), all local density approximations except for MODA involve derivatives of the pair distribution functions (of the uniform system) with respect to the densities. (Within the LADA approach, even the second derivatives appear.)

Alternatively, the square-gradient term may be calculated from the direct correlation functions (also of the homogeneous system) according to [26]

$$\phi_{i,\nabla^2}^{\text{res}}(\mathbf{r}) = \frac{\sigma^3}{12} \sum_k \int r_{ik}^2 C_{ik}(r_{ik}) \, d\mathbf{r}_{ik} \, \nabla \rho_i(\mathbf{r}) \cdot \nabla \rho_k(\mathbf{r}). \quad (5)$$

Here and in the following equations, we omit the temperature and density dependence of the correlation functions for notational simplicity and retain the interparticle distance as the only argument. Note that (5) involves no local density approximation because it relies on the reasonable assumption that the density does not change appreciably within the range of the direct correlation function [27]. This is to be contrasted with the situation for the much longer-ranged pair distribution function. In principle, however, one could devise LADA or DAPA versions of this equation as well when replacing the unknown direct correlation function of the inhomogeneous system as defined by the second functional derivative of the free-energy functional by the approximately known direct correlation function of the homogeneous system.

The direct correlation function is related rigorously to the total correlation function $h_{ik} = g_{ik} - 1$ via the Ornstein–Zernike relation [28]:

$$h_{ik}(r_{ik}) = C_{ik}(r_{ik}) + \sum_j \rho_j \int C_{ij}(r_{ij}) h_{jk}(r_{jk}) \, d\mathbf{r}_j. \quad (6)$$

Given a particular pair potential u_{ik} , the unknown correlation functions C_{ik} and h_{ik} can only be calculated if a second equation relating them, the closure, is assumed or postulated. The most prominent closure relations are the MSA, the Percus–Yevick (PY) closure and the hypernetted-chain (HNC) relation, which is given by [28]

$$C_{ik} = -\beta u_{ik} + h_{ik} - \ln(1 + h_{ik}). \quad (7)$$

This can be further approximated by expanding the logarithm in powers of h_{ik} and truncating this series after the quadratic term to give

$$C_{ik} = -\beta u_{ik} + \frac{1}{2} h_{ik}^2. \quad (8)$$

We will use this approximate (A)HNC relation as a shortcut from the known h_{ik} (within DH and FL theory [29]) to the square-gradient term.

A third approach, used by Lee and Fisher in their GDH theory, obtains the direct correlation functions by functional differentiation of the free energy of the inhomogeneous system [20].

Note that using the AHNC relation or the GDH theory does not necessarily require a local density approximation as the square-gradient term is calculated via the direct correlation function from a theory for the bulk fluid.

For any given u_{ik} and g_{ik} or h_{ik} , both contributions to the local free-energy density as given in (3) and (4) or (5) can now be calculated. The next subsection explains how this gradient theory is used to compute the interfacial properties of interest to us.

2.2. Interfacial properties within square-gradient theory

As outlined in the previous subsection, the local free energy of the system now consists of the homogeneous part and the square-gradient contribution: $\phi(\mathbf{r}) = \phi_{\text{hom}}(\mathbf{r}) + \phi_{\nabla^2}(\mathbf{r})$. The first quantity of interest that we can calculate within this square-gradient mean-field theory is the second moment (Ornstein–Zernike) correlation length, which, in units of σ , is

$$\xi^* = \xi/\sigma = \left[c \left(\frac{\partial^2 \phi_{\text{hom}}}{\partial \rho^{*2}} \right)^{-1} \right]^{1/2}. \quad (9)$$

Here, c is the coefficient of the square-gradient term as it appears in $\phi_{\nabla^2} = c(\nabla^* \rho^*)^2$ and $(\partial^2 \phi_{\text{hom}}/\partial \rho^{*2})^{-1}$ is the susceptibility (compressibility) of the system.

As outlined in detail elsewhere [30], the density profile across the liquid–vapour interface can be found from

$$\int_{\rho_0^*}^{\rho^*} \left(\frac{T^* c(\rho^*)}{2 \Delta \omega(\rho^*)} \right)^{1/2} d\rho^* = -z/\sigma = -z^* \quad (10)$$

where z is the coordinate perpendicular to the planar liquid–vapour interface. In the above equation, ρ^* denotes $\rho^*(z^*)$, the spatially varying density in the interface. ρ_0^* is the density at $z^* = 0$ taken to be the arithmetical mean of the densities in the liquid phase and in the vapour phase: $\rho_0^* = \rho^*(z^* = 0) = (\rho_l^* + \rho_v^*)/2$. The quantity $\Delta \omega(\rho^*)$ is defined by $\Delta \omega(\rho^*) = \omega(\rho^*) + P_{\text{bulk}}^*$. The reduced bulk pressure is introduced via $P_{\text{bulk}}^* = P_{\text{bulk}} \varepsilon \sigma^4 / q^2$ for the RPM. $\omega(\rho^*) = T^*(\phi_{\text{hom}}(\rho^*) - \rho^* \mu_{\text{bulk}}^*)$, where $\mu_{\text{bulk}}^* = \beta \mu_{\text{bulk}}$ denotes the reduced bulk chemical potential, varies with the local density and, therefore, across the interface. P_{bulk}^* and μ_{bulk}^* are obtainable from ϕ_{hom} . The above expression (10) is derived by minimizing the square-gradient free-energy functional

$$I(\{\rho^*\}) = \int_{-\infty}^{+\infty} \left[\Delta \omega(\rho^*) + \frac{1}{2} T^* c(\rho^*) \left(\frac{\partial \rho^*}{\partial z^*} \right)^2 \right] dz^* \quad (11)$$

using the Euler–Lagrange equation [27, 30, 31]. Within gradient theory, the two terms in the integrand of (11) measure the gain and loss of free-energy density when a certain density profile is established. The interplay of these contributions determines, via the minimization condition, the equilibrium density profile, which represents a compromise between the penalties in the free energy caused by having densities different from a bulk density on the one hand and by introducing a density gradient on the other hand. The minimization condition is equivalent to imposing that the chemical potential be constant throughout the system [31]. The dimensionless surface tension $\gamma^* = \gamma \varepsilon \sigma^3 / q^2$ is obtained from

$$\gamma^* = \int_{\rho_v^*}^{\rho_l^*} \sqrt{2 T^* c(\rho^*) \Delta \omega(\rho^*)} d\rho^*. \quad (12)$$

In addition to this quantity, we define the reduced interfacial tension $\bar{\gamma} = \gamma^* / T_c^* = \beta_c \gamma \sigma^2$.

Another quantity of interest is the thickness of the interface, which we will simply take as the ‘10–90’ thickness, i.e. the distance over which the density varies from $\rho_v^* + 0.1(\rho_l^* - \rho_v^*)$ to $\rho_v^* + 0.9(\rho_l^* - \rho_v^*)$.

2.3. Application of the formalism to the RPM

As mentioned in the introduction, we will first account for the thermodynamic properties of the RPM by the DH theory, which considers only the interactions of free ions (II), and then, as an improvement over DH theory, by the FL theory. Here, following basically the ideas of Bjerrum, the ions form pairs, which themselves represent dipolar particles that, in turn, interact with the free ions. This dipole–ion (DI) interaction is treated in a DH-style approach [14].

In both theories, the hard-sphere contribution is neglected because of the low densities. The ideal-gas contribution of species i is given by

$$\phi_i^{\text{id}} = \rho_i^* [\ln(\rho_i \Lambda_i^3) - 1] \tag{13}$$

where Λ_i denotes the thermal de Broglie wavelength. The residual term is calculated from (3), with u_{ik} and g_{ik} as appropriate for the II interaction within DH theory:

$$u_{ik}^{\text{II}}(r_{ik}) = \frac{q_i q_k}{\epsilon r_{ik}} \tag{14}$$

$$g_{ik}^{\text{II}}(r_{ik}) = 1 - \beta \frac{q_i q_k e^{\kappa(\sigma - r_{ik})}}{\epsilon r_{ik} (1 + \kappa \sigma)}. \tag{15}$$

Here κ is the inverse Debye length and, with $x = \kappa \sigma = (4\pi \rho_i^* / T^*)^{1/2}$, the well-known result for $\phi_{\text{hom}}^{\text{res}}$ within DH theory is

$$\phi_{\text{hom}}^{\text{res,II}} = -\frac{1}{4\pi} \left[\ln(1 + x) - x + \frac{1}{2}x^2 \right]. \tag{16}$$

The square-gradient term is computed according to (4) within the extended van der Waals approach. The coefficient c of this term may be represented as [23]

$$c = c_0 + a_1 c_1 + a_2 c_2 \tag{17}$$

with

$$c_0 = \frac{1}{12\pi \rho_i^{*2}} \left[\ln(1 + x) + x + \frac{1}{2}x^2 \right] \tag{18}$$

$$c_1 = -\frac{1}{24\pi \rho_i^{*2}} \frac{2x + 4x^2 + x^3 + 4(1 + x) \ln(1 + x)}{1 + x} \tag{19}$$

$$c_2 = \frac{1}{48\pi \rho_i^{*2}} \frac{6x + 24x^2 + 23x^3 + 4x^4 + 24(1 + x)^2 \ln(1 + x)}{(1 + x)^2} \tag{20}$$

where the term c_n arises from the n th derivative of the pair distribution function with respect to density. The different local density approximations used in the expansion lead to different prefactors a_1 and a_2 . While the MODA approach involves no derivative with respect to density, i.e. $a_1 = a_2 = 0$, BAPA and DAPA contain terms from the first derivative and therefore have $a_1 = 2/3$ and $a_1 = 1/2$, respectively, while still $a_2 = 0$. Within LADA, even the second derivative appears and leads to $a_1 = 1$ and $a_2 = 1/4$.

The AHNC relation yields [23]

$$c_{\text{AHNC}} = \frac{\pi}{12} \frac{1 + 2x + 2x^2}{x^3 T^{*2} (1 + x)^2} \tag{21}$$

via (5), whereas the GDH theory gives [20]

$$c_{\text{GDH}} = \frac{1}{96\pi \rho_i^{*2}} \left[\ln \left(\frac{(1 + x)^{10}}{(1 + x + \frac{1}{3}x^2)^9} \right) - \frac{x - 5x^2 - 8x^3}{2(1 + x)^2} \right]. \tag{22}$$

The last two expressions for the coefficient c yield rather similar results, which can be demonstrated by expanding the logarithm in (22), casting the result into the form of (21), and comparing just the numerators of the second fraction. The GDH result $1 + 2x + 8x^2/3 + O(x^3)$ is identical to the AHNC expression to order $O(x)$. This fact will be important when we consider the low-density limit. The local density approximations MODA, LADA and DAPA, however, differ already in the leading x^0 -term by yielding coefficients of 32, 14 and 8, respectively, instead of unity. The BAPA approach represents an exception; here, the leading term is $32x^2/9$, which causes a pathological behaviour at very low densities. The consequences of this behaviour for the correlation length in the dilute vapour phase and the asymmetry of the resulting density profile have been explained in detail elsewhere [23].

Now, with the above expressions, the interfacial properties and the correlation length can be calculated in the framework of DH theory; the results are given in section 3.1.

For the FL theory, things are a bit more complicated. First, in this chemical picture, the fluid is regarded as a reacting mixture of free ions and ion pairs. The total ionic density, which is the thermodynamically relevant quantity, is given by $\rho = \rho_i + 2\rho_p$, where ρ_i , as before, denotes the density of free ions and ρ_p that of pairs. Within FL theory [14], the ion pairs are assumed to be of spherical shape with a diameter of $\sigma_2 = a\sigma$, with $a = 1.162$, and to possess a dipole moment of magnitude $\mu = q\sigma$. While the II contribution to the free-energy density remains the same as in DH theory, the dipole-ion part is given by [14]

$$\phi_{\text{hom}}^{\text{DI}} = -\frac{3\rho_p^*}{a^5 x^2 T^*} \left[\ln \left(1 + ax + \frac{1}{3} a^2 x^2 \right) - ax + \frac{1}{6} a^2 x^2 \right]. \quad (23)$$

This result is also obtained from (3) using the appropriate interaction potential and pair distribution function [29]:

$$u_{ik}^{\text{DI}}(r_{ik}) = \frac{q_i \mu_k}{\epsilon r_{ik}^2} \hat{r}_{ik} \cdot \hat{\mu} \quad (24)$$

$$g_{ik}^{\text{DI}}(r_{ik}) = 1 - \beta \frac{q_i \mu_k}{\epsilon r_{ik}^2} \hat{r}_{ik} \cdot \hat{\mu} \frac{(1 + \kappa r_{ik}) e^{\kappa(a\sigma - r_{ik})}}{1 + ax + \frac{1}{3} a^2 x^2} \quad (25)$$

where the circumflexes denote unit vectors. To determine the degree of ion pairing, an association equation derived from the mass action law for pairs in equilibrium with free ions [14] is used:

$$\rho_p^* = \frac{\rho_i^{*2}}{4} K(T^*) e^{2\mu_i^{*\text{ex}} - \mu_p^{*\text{ex}}}. \quad (26)$$

Here, $\mu_j^{*\text{ex}}$ is the reduced excess chemical potential and $K(T^*)$ denotes the association constant, for which we choose a truncated Bjerrum expression:

$$K(T^*) = 4\pi e^{1/T^*} T^* \sum_{n=3}^9 \frac{n!}{3!} (T^*)^{n-3}. \quad (27)$$

These equations completely specify the homogeneous part of the free energy within FL theory. When evaluating formula (12) for γ^* (using e.g. Simpson's rule), the total density ρ at any particular point of interest along the z -axis has to be divided up into the ionic density ρ_i and the pair density ρ_p according to the association equation (26).

The square-gradient term also involves contributions from ion-ion (II) interactions and from dipole-ion (DI) interactions. For the MODA treatment and the AHNC relation, only g^{II} contributes to the coefficient $c^{\text{II}} = 2\phi_{\nabla^2}^{\text{II}}/(\nabla^* \rho_i^*)^2$, while $c^{\text{DI}} = 2\phi_{\nabla^2}^{\text{DI}}/\nabla^* \rho_i^* \cdot \nabla^* \rho_p^*$ is determined by g^{DI} . Since the coefficient c corresponds to the square-gradient of the total density,

$(\nabla^* \rho^*)^2$, the individual c^{ik} have to be weighted according to factors $(\partial \rho_i / \partial \rho)_T (\partial \rho_k / \partial \rho)_T$. Thus, we obtain the overall coefficient from

$$c = c^{\text{II}} \left(\frac{\partial \rho_i}{\partial \rho} \right)_T^2 + c^{\text{DI}} \left(\frac{\partial \rho_i}{\partial \rho} \right)_T \left(\frac{\partial \rho_p}{\partial \rho} \right)_T. \quad (28)$$

Explicitly, from the AHNC relation, we find

$$c^{\text{II}} = \frac{\pi}{12} \frac{1 + 2x + 2x^2}{T^{*2} x^3 (1 + x)^2} \quad (29)$$

$$c^{\text{DI}} = \frac{\pi}{4} \frac{5 + 6ax + 2a^2 x^2}{T^{*2} x (3 + 3ax + a^2 x^2)^2}. \quad (30)$$

When local density approximations like DAPA, LADA or BAPA are used to compute the square-gradient term, there will also be contributions from g^{DI} to the coefficient c^{II} , as can be seen from (4). Due to the appearance of the derivative of g^{DI} (which depends on ρ_i via κ) with respect to ρ_i , there arise nonzero terms corresponding to a square-gradient $(\nabla \rho_i)^2$. The formulae that we obtained for these treatments are, however, too lengthy to be displayed here.

Now we are prepared to calculate the interfacial properties of the RPM within DH and FL theory. In figure 1, the coexistence curves following from these two theories are shown. First, the densities of coexisting phases can be read off from this diagram, and, second, it clearly demonstrates that the FL theory represents a substantial improvement over DH theory in that it yields very good agreement with simulation results for the coexistence curve of the RPM. The DH curve is much too narrow, leading to density differences between the liquid phase and the vapour phase which are too small. To obtain reasonable estimates for the surface tension, it is crucial to employ the FL theory instead of DH theory. (We have refrained from including the MSA coexistence curve in figure 1, because, due to the high critical temperature within the MSA, the region that we will focus on in this paper would appear unduly compressed in the picture.)

3. Results and discussion

In this section, we will first investigate the implications of the local density approximations for the interfacial properties within the Debye–Hückel theory. Subsequently, the results within the more accurate Fisher–Levin theory are presented and, finally, compared with findings in earlier studies of the liquid–vapour interface of ionic fluids which were also based on the RPM.

3.1. Debye–Hückel theory

The results for the density profiles and interfacial tensions within DH theory have already been given elsewhere [23], but, as they are relevant to the discussion and the assessment of the results from FL theory, we will summarize the major points here.

Figure 2 shows the density profiles obtained from the different methods to compute the square-gradient term within DH theory at a temperature of $T^* = 0.05$ (or $T/T_c = 0.8$). Except for the one following from the BAPA treatment (see [23]), the density profiles are rather symmetric; however, they differ significantly in the predicted thickness of the interface: while, using the AHNC relation, the ‘10–90’ thickness is merely four molecular diameters, the interface extends over 20σ in the MODA approach. Equally dramatic are the differences in the surface tensions, which are given in table 1. The tension obtained from MODA is five times higher than the one from the AHNC relation, while the other treatments yield values intermediate between these extremes. Nevertheless, even the most reasonable approximations

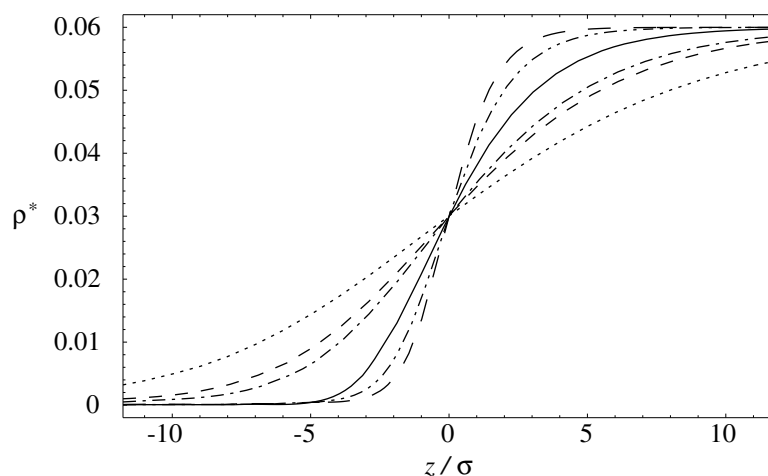


Figure 2. Density profiles for an ionic model fluid within Debye–Hückel theory at a temperature of $T^* = 0.05$ or $T/T_c = 0.8$. The profile is shown for various approximations to the local density: MODA (dotted), LADA (short-dashed), DAPA (dash–dotted), BAPA (continuous), for the GDH theory (dash–dot–dotted) and for the approach via the AHNC relation (long-dashed). The abbreviations for the different local density approximations are explained in the main text.

Table 1. Results obtained within DH theory from the listed local density approximations, as defined in section 2.1, the GDH theory and the AHNC relation, respectively, for the reduced surface tension $\bar{\gamma} = \beta_c \gamma \sigma^2$ and the correlation length in the liquid and in the vapour phase at $T^* = 0.05$ ($T/T_c = 0.8$). In addition, the square of the prefactor a_ξ of the exact Lee–Fisher result for ξ in the low-density limit is given.

Approximation	$\bar{\gamma}$	ξ_l^*	ξ_v^*	a_ξ^2
MODA	0.0546	5.565	14.48	32
LADA	0.0370	3.833	9.586	14
DAPA	0.0305	3.429	7.259	8
BAPA	0.0151	2.314	0.581	0
GDH	0.0125	1.395	2.587	1
AHNC	0.0102	0.971	2.574	1

to the local density, DAPA and LADA, still differ by a factor of three or four, respectively, from the AHNC result. Which one is to be believed? Help in reaching a decision comes from the behaviour of the correlation length in the low-density limit. Lee and Fisher found from their GDH theory the correct leading behaviour to be $\xi = (b/9216\pi\rho)^{1/4}$, where $b = \sigma/T^*$ is the Bjerrum length [20]. Qualitatively, this expression is also found within the other approaches to the square-gradient term (except for the BAPA method), differing, however, by a numerical coefficient in front of the exact Lee–Fisher expression, which we denote by a_ξ . This coefficient has already been alluded to in section 2.3, where we compared the expansions of the various results for the square-gradient term. As is seen in table 1, MODA, LADA and DAPA predict correlation lengths in the low-density limit which are too large by factors of $\sqrt{32}$, $\sqrt{14}$ and $\sqrt{8}$, respectively. Obviously, these factors also appear, with only minor changes, at finite densities, i.e. in the values of the correlation lengths in the coexisting phases ξ_l and ξ_v (cf. table 1). Since $4\xi_l$ gives a good estimate of the interfacial thickness [25], these factors are also visible in the width of the density profiles as well as in the values of the surface tension due to both quantities being proportional to $c^{1/2}$. The AHNC relation, like the GDH theory, gives the exact

expression and, thus, the correct value of $a_\xi = 1$.

From these observations, we are forced to conclude that the local density approximations LADA and DAPA, which at first sight appear most reasonable, cannot be trusted for ionic fluids (within DH theory) as they overestimate the thickness of the interface and the interfacial tension by a factor of three [23]. Most reliable appear the AHNC relation and the GDH theory, as they require no local density approximation, lead to the correct behaviour of ξ in the low-density limit and are self-consistent in a sense that the compressibility calculated from the respective direct correlation functions that they predict equals the one obtained from differentiating the free-energy density twice with respect to density.

The above comparison was only relative in nature; in general, we cannot expect to obtain good absolute numerical estimates of the surface tension in the RPM from such an inaccurate theory as the DH theory. The narrow coexistence curve within DH theory (cf. figure 1) leads to too small a difference $\rho_l - \rho_v$ and, thus, we must suspect that the values of $\bar{\gamma}$ given in table 1 are also too low. To remove this shortcoming, we will now examine the interfacial properties within FL theory.

3.2. Fisher–Levin theory

In the present analysis, we will restrict ourselves to the AHNC relation, which is computationally significantly less demanding than the GDH theory while still yielding similar results [22, 23], and to the DAPA treatment in order to check by means of an example whether the above statements on the sensitivity of the correlation length and the interfacial properties to the local density approximation within DH theory remain valid for the FL theory.

The results for the reduced surface tension $\bar{\gamma} = \gamma^*/T_c^* = \beta_c \gamma \sigma^2$ are given in table 2 along with the correlation lengths in the coexisting phases. We have compiled the predictions of the AHNC and the DAPA treatments within FL theory at a reduced temperature of $T/T_c = 0.8$ and those within DH theory for comparison. Since, as we will argue in the following, the AHNC-FL theory must be regarded as the most trustworthy one, we have calculated the interfacial properties for this theory at other temperatures ($T/T_c = 0.9, 0.95$) as well. These values are to be compared with the results of Groh *et al* [25] from their study based on density-functional theory, which uses the MSA in conjunction with the LADA, in section 3.3. The density profiles that we obtained for the AHNC-FL theory at $T/T_c = 0.8, 0.9, 0.95$ are shown in figure 3 along

Table 2. Reduced correlation length in the liquid phase ξ_l^* and in the vapour phase ξ_v^* as well as reduced surface tension $\bar{\gamma} = \beta_c \gamma \sigma^2$ for different temperatures as obtained from the AHNC relation or the DAPA method, respectively, in conjunction with either the Fisher–Levin (FL) or the Debye–Hückel (DH) theory. For comparison, we have also compiled the results of Groh *et al* from their LADA-MSA1 treatment [25] and the density differences of the coexisting phases $\rho_l^* - \rho_v^*$ at the respective temperatures for all three theories.

Approximation	T^*	T/T_c	ξ_l^*	ξ_v^*	$\bar{\gamma}$	$\rho_l^* - \rho_v^*$
AHNC-FL	0.0459	0.8	1.19	0.82	0.030	0.325
AHNC-FL	0.0517	0.9	1.64	1.60	0.0086	0.125
AHNC-FL	0.0545	0.95	2.27	2.44	0.0028	0.065
DAPA-FL	0.0459	0.8	3.40	1.92	0.073	0.325
AHNC-DH	0.05	0.8	0.97	2.57	0.010	0.060
DAPA-DH	0.05	0.8	3.43	7.26	0.031	0.060
LADA-MSA1	0.0677	0.8	1.6	6.1	0.037	0.092
LADA-MSA1	0.0761	0.9	2.5	5.3	0.015	0.054
LADA-MSA1	0.0804	0.95	3.6	5.9	0.006	0.035

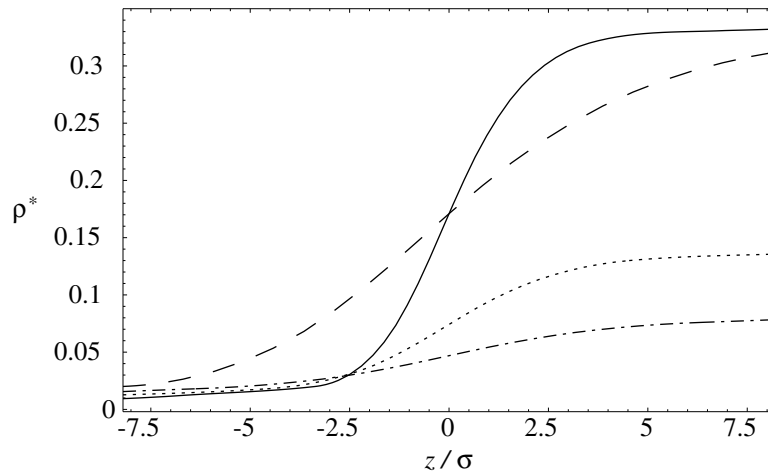


Figure 3. Density profiles across the liquid–vapour interface within Fisher–Levin theory at different temperatures. The square-gradient term has been calculated using an approximate hypernetted-chain relation (AHNC) or a local density approximation (DAPA; see the main text): AHNC at $T/T_c = 0.8$ (continuous), AHNC at $T/T_c = 0.9$ (dotted), AHNC at $T/T_c = 0.95$ (dash-dotted) and DAPA at $T/T_c = 0.8$ (long-dashed).

with the one that results from the DAPA-FL treatment at $T/T_c = 0.8$.

To start with these profiles, it is seen from figure 3 that, at a temperature of $T/T_c = 0.8$, the profile obtained from DAPA-FL theory (long-dashed) is about three times broader than the one following from the AHNC-FL theory (continuous); the ‘10–90’ thickness at this temperature is about 5σ within AHNC-FL theory compared to 14σ for the DAPA-FL treatment. So, the interfacial thickness is about the same as the one found within DH theory for both approaches, AHNC and DAPA. The same is true for the correlation length in the liquid phase: AHNC-FL theory leads to $\xi_l^* = 1.19$ compared to $\xi_l^* = 0.97$ within DH theory, while the DAPA-FL theory gives $\xi_l^* = 3.40$ which is almost the same as the DAPA-DH result of $\xi_l^* = 3.43$. Thus, again, in all cases the thickness of the interface is given by $4\xi_l$. Furthermore, it is clearly seen that choosing a particular local density approximation like DAPA leads to an almost density-independent and, thereby, constant factor of three compared to the results from the AHNC relation, which persists from the behaviour of ξ in the low-density limit to ξ_l and, consequently, to the interfacial thickness at finite densities. This is observed in DH theory as well as in FL theory. From AHNC-DH to AHNC-FL theory, the reduced surface tension $\bar{\gamma}$ increases by a factor of three. This increase must be attributed to the larger density difference $\rho_l - \rho_v$ in the FL theory (cf. table 2).

Because of the behaviour in the low-density limit, we trust the results from the AHNC relation rather than those from the DAPA treatment. This is why we compute the interfacial properties of the RPM at different temperatures only for the AHNC-FL theory. From figure 3, it is seen that, as expected, the density profile broadens as the critical temperature is approached. At the same time, the surface tension decreases and vanishes asymptotically near the critical point as $\bar{\gamma} \sim (1 - T/T_c)^{3/2}$ within a mean-field theory such as the present one. According to our calculations, a description in terms of this asymptotic power law is, however, only appropriate for $T/T_c > 0.98$, a region in which mean-field theory ceases to be valid anyway. As the critical point is approached from $T/T_c = 0.8$ within AHNC-FL theory, the correlation length increases, with the interfacial thickness still given by $4\xi_l$. At $T/T_c = 0.9$ the correlation

lengths in the coexisting phases are almost equal, while we have $\xi_v < \xi_l$ for $T/T_c < 0.9$ and $\xi_v > \xi_l$ for $T/T_c > 0.9$. Accordingly, the asymmetry of the density profiles is inverted at this temperature. While for $T/T_c < 0.9$ the decay to the bulk density is more rapid on the vapour side, the opposite is the case for $T/T_c > 0.9$. Within square-gradient theory, the asymmetry of the profile is determined by whether $\xi_v < \xi_l$ (yielding a more rapid decay to the bulk density on the vapour side) or $\xi_v > \xi_l$ (leading to the opposite asymmetry of the profile). Telo da Gama *et al* [32] studied the RPM using the GMSA in a square-gradient theory and found a more rapid decay on the liquid side for all temperatures, which is in accordance with our results from DH theory (except for the pathological BAPA case). The opposite behaviour was found by Groh *et al* [25] in their study based on the MSA and density-functional theory. Here, within AHNC-FL theory, the asymmetry turns out to be temperature dependent due to the change of the correlation lengths in both phases. We will take this opportunity to compare the variation of the correlation length along the coexistence curve within the AHNC-FL and AHNC-DH theories. The results are shown in figure 4. Whereas ξ_l is expected to decay monotonically when moving away from the critical point, as seen in figure 4 for both the FL theory (dash-dotted) and the DH theory (continuous), the behaviour on the vapour side of the coexistence curve is different for ionic fluids. Within DH theory, ξ_v (dotted) passes through a minimum as it diverges both at the critical point and in the low-density limit (according to the Lee–Fisher expression; see above). This is true when ionic association is neglected, as is done in DH theory. Along the vapour branch of the coexistence curve, both the density and the temperature decrease, but, according to the Lee–Fisher result, lowering the temperature as $\rho \rightarrow 0$ even increases ξ . In association theories, such as the present FL theory, there is a competition in the low-density, low-temperature phase between the dissociation process, favoured by the low density, and the association process, which is favoured by low temperatures. Which of these tendencies will ultimately prevail is expected to depend on the theory used in the computations. Within FL theory in connection with the Bjerrum association constant (27), the numerical evidence that we obtained for the region $0.5 < T/T_c < 1$ points towards a nearly

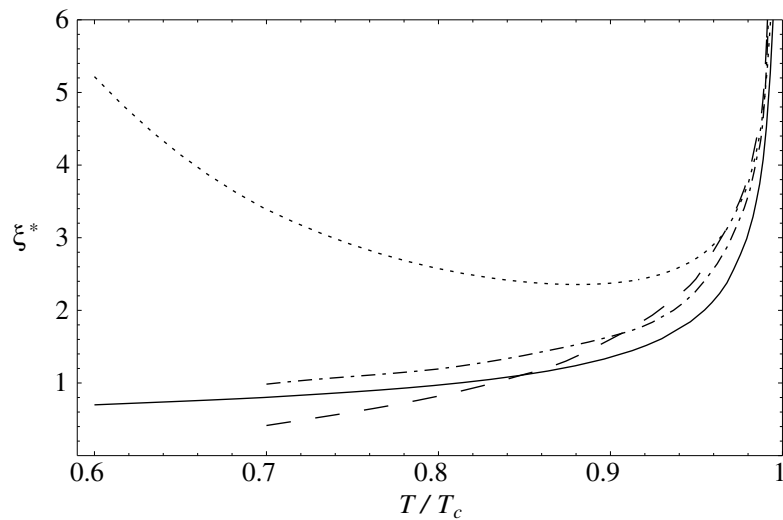


Figure 4. Correlation lengths in the liquid phase and in the vapour phase within Debye–Hückel (DH) theory and Fisher–Levin (FL) theory, respectively, in conjunction with the AHNC relation. DH: ξ_v^* (dotted), ξ_l^* (continuous); FL: ξ_v^* (long-dashed), ξ_l^* (dash-dotted).

complete depletion of free ions in the low-temperature vapour phase. This in turn means that, in the end, there are no free ions left which could cause ξ_v to diverge according to the Lee–Fisher expression in the low-density, but also low-temperature limit. This ultimate behaviour is, however, purely hypothetical within a theory for the fluid phases as the line of liquid–vapour equilibrium terminates at the triple point, which, for the RPM, has been estimated to be located at $T_{tr}^* = 0.025$ and $\rho_{tr}^* = 0.5$ [33]. In addition to this, we cannot recommend employing the FL theory in its present form at reduced temperatures below $T/T_c = 0.7$, since then the density of the liquid phase becomes unrealistically high and hard-sphere contributions can no longer be neglected. In summary, we may state that while for the AHNC-DH theory ξ_v is always larger than ξ_l , for the AHNC-FL treatment ξ_v drops below ξ_l for $T/T_c < 0.9$ (cf. figure 4) due to pronounced ion pairing in the vapour phase. The formation of dipolar ion pairs reduces ξ_v as compared to the correlation length in the vapour phase within DH theory; ξ_l , in contrast, remains almost the same (see table 2), as the degree of ion pairing is not that high in the liquid phase. While there is no minimum of ξ_v within AHNC-FL theory, the one found in AHNC-DH theory is located at $T/T_c = 0.9$. Very much the same numerical value was found in the MSA-based treatment of Groh *et al* [25].

3.3. Comparison with results of earlier studies

As mentioned in the introduction, Groh *et al* employ the MSA in conjunction with the LADA to obtain results for the interfacial properties and the correlation length in their density-functional theory, which goes beyond the square-gradient approximation. The standard MSA (probably incorrectly) leads to effective potentials for the density–density correlations which decay algebraically for large separations, whereas the density–density correlation function is expected to decay exponentially in this limit [34,35]. As a remedy, Groh *et al* introduce the MSA variant ‘MSA1’, in which, in contrast to the standard MSA, the thermodynamic integration (or, for ionic fluids, the charging process) is left out. Doing so amounts to replacing the residual free energy by the configurational internal energy that is due to ion–ion interactions. Within this MSA1, the decay of the above-mentioned functions is indeed exponential [25]. As Groh *et al* [25] show, the differences with respect to the coexistence curve between MSA and MSA1 are minor; both approaches overestimate the critical temperature significantly and the agreement of the coexistence curves with results from simulations is not satisfactory. The omission of the thermodynamic integration in MSA1 leads to a prefactor of $a_\xi = \sqrt{7}$ in front of the Lee–Fisher expression for ξ in the low-density limit, instead of the $\sqrt{14}$ expected for the LADA treatment employed. (In the low-density limit, the correlation functions predicted by the MSA and the DH theory become identical, so they give the same a_ξ for a chosen local density approximation.) So, if it were possible to extrapolate the factor a_ξ arising from different approximations to the local density in the correlation length in the low-density limit to the properties at finite densities, which worked so well for the DH theory, within this MSA-based density-functional theory, we would expect the surface tension obtained from the MSA to be larger than that from MSA1 by a factor of about $\sqrt{14}/\sqrt{7} = \sqrt{2}$. Indeed, the presence of such a factor can be seen in figure 6 of the paper by Groh *et al* [25], in which the surface tensions resulting from MSA and MSA1 are compared. In fact, the observed factor is even larger than $\sqrt{2}$ —about 1.6—due to a larger difference $\rho_l - \rho_v$ at the same T/T_c for the MSA, which has a lower critical temperature. It is difficult to separate the two contributions, but it can safely be stated that both mechanisms are at work here. This observation strongly suggests that extrapolation from the low-density limit is approximately valid and that the MSA has the same sensitivity towards the local density approximation as the DH-based theories (although this has not been checked explicitly). We therefore argue that our results from the AHNC-

FL theory are more reliable, at least in a temperature range in which the density gradient is small, say, for $0.85 \leq T/T_c \leq 0.95$. Closer to the critical point, mean-field theory will fail. The only weakness of our approach is the simple density functional in the square-gradient theory; the thermodynamic description by FL theory is reliable and the AHNC route to the square-gradient term apparently as well. Groh *et al* use a thermodynamic theory (MSA or MSA1) that cannot be considered to give an accurate account of the properties of the RPM (as judged from the coexistence curve) and the use of the LADA is at least questionable for ionic fluids. A point in favour of their work is that they employ a more elaborate nonlocal density-functional approach. The main intention of the work of Groh *et al*, however, was to obtain information from the MSA, which works so well in many other cases, but in the context of interfacial properties turns out to be useless if employed in ‘standard’ ways. So, it was not their primary goal to obtain the best-possible numerical estimates for the interfacial properties. Consequently, they only claim that their results give the right order of magnitude, which is certainly in accordance with our results and the ones found by Telo da Gama *et al* [32] from their GMSA-based study. The accuracy of the results from the latter approach is limited by the restriction to small gradients due to the square-gradient theory employed and, additionally, by using the GMSA, which yields a coexistence curve that is almost identical to the one obtained from the MSA. On the other hand, within the GMSA, there is no doubt about the correct route to the square-gradient term via the direct correlation function and, therefore, also no need to introduce a local density approximation. The approach of Groh *et al* generally leads to larger results for the interfacial tension than the GMSA square-gradient treatment at the same reduced temperature [25]. Furthermore, within the standard MSA (as opposed to the MSA1), the interfacial tensions are twice as high as within the GMSA [25], closer to the critical point even three times higher. This, again, points to an overestimation of $\bar{\gamma}$ that might be due to the use of the LADA, given that the coexistence curves are almost identical. In contrast, the predictions of the GMSA and the AHNC-FL theory agree very well, with the GMSA values being slightly larger. For $T/T_c \leq 0.85$, the relatively large values of $\rho_l - \rho_v$ combined with the small interfacial thickness at these temperatures result in gradients which might be too large to render the square-gradient theory valid. In this temperature region the results of the LADA-MSA1 and the AHNC-FL differ only by 20%, which may be accidental. At higher temperatures, however, the results from AHNC-FL theory are smaller by a factor of two compared to the LADA-MSA1 results (cf. table 2). Here, the gradient is smaller; thus, square-gradient theory should be valid, and we tend to trust the AHNC-FL results more on the grounds of the arguments outlined above.

4. Conclusions

We have calculated interfacial tensions and density profiles for the liquid–vapour interface of the RPM of ionic fluids within the currently most successful theory for the thermodynamic properties of the RPM, the Fisher–Levin theory, and a relatively simple square-gradient theory. It was observed that within DH theory and its extension, the FL theory, one has to choose carefully the method by which to compute the square-gradient term. For different local density approximations, the results for the surface tension and the interfacial thickness may vary by factors of 3–5. A guideline to a reliable local density approximation or, alternatively, to a reliable approximate direct correlation function, from which the square-gradient term can be calculated, is provided by the behaviour of the correlation length in the low-density limit. Here, we rely on the computationally simple to use AHNC relation for the direct correlation function. The GDH theory of Lee and Fisher [20] would, in principle, also be appropriate, but is mathematically more demanding than the AHNC route. Both the AHNC relation and the

GDH theory yield correct results in the low-density limit and are ‘self-consistent’ within the DH theory in the sense specified above.

From our approach, which to our knowledge is the first attempt to compute the interfacial properties of an ionic fluid within an association theory, we expect to obtain reliable results for the temperature range $0.85 \leq T/T_c \leq 0.95$, in which the gradient is not too large. To arrive at more accurate results at lower temperatures, one could, of course, improve upon the simple square-gradient theory by using a more elaborate nonlocal density-functional theory. Unfortunately, there appear to be no simulations for the RPM against which to check our results. The molecular-dynamics study by Heyes and Clarke uses the more realistic Born–Mayer–Huggins potential model and is concerned with rather low temperatures [36]. Nevertheless, we believe that the AHNC-FL square-gradient theory offers a promising and tractable approach to the interfacial properties of ionic fluids.

Acknowledgments

Helpful discussions with R Evans, M E Fisher, B Groh, M Kleemeier, G Stell, B P Vollmayr-Lee, B Widom and S Wiegand are appreciated.

References

- [1] Singh R R and Pitzer K S 1990 *J. Chem. Phys.* **92** 6775
- [2] Zhang K C, Briggs M E, Gammon R W and Levelt Sengers J M H 1992 *J. Chem. Phys.* **97** 8692
- [3] Wiegand S, Levelt Sengers J M H, Zhang K J, Briggs M E and Gammon R W 1997 *J. Chem. Phys.* **106** 2777
Wiegand S, Briggs M E, Levelt Sengers J M H, Kleemeier M and Schröer W 1998 *J. Chem. Phys.* **109** 9038
- [4] Narayanan T and Pitzer K S 1995 *J. Chem. Phys.* **102** 8118
- [5] Panagiotopoulos A Z 1992 *Fluid Phase Equilibria* **76** 97
- [6] Caillol J M 1994 *J. Chem. Phys.* **100** 2161
- [7] Orkoulas G and Panagiotopoulos A Z 1994 *J. Chem. Phys.* **101** 1452
- [8] Fisher M E 1994 *J. Stat. Phys.* **75** 1
Fisher M E 1996 *J. Phys.: Condens. Matter* **8** 9103
- [9] Stell G 1995 *J. Stat. Phys.* **78** 197
Stell G 1996 *J. Phys.: Condens. Matter* **8** 9329
- [10] Caillol J M and Weis J J 1995 *J. Chem. Phys.* **102** 7610
- [11] Bresme F, Lomba E, Weis J J and Abascal J L F 1995 *Phys. Rev. E* **51** 289
- [12] Yeh S, Zhou Y and Stell G 1996 *J. Phys. Chem.* **100** 1415
Zhou Y, Yeh S and Stell G 1995 *J. Chem. Phys.* **102** 5785
- [13] Guillot B and Guissani Y 1996 *Mol. Phys.* **87** 37
- [14] Fisher M E and Levin Y 1993 *Phys. Rev. Lett.* **71** 3826
Levin Y and Fisher M E 1996 *Physica A* **225** 164
- [15] Weiss V C and Schröer W 1998 *J. Chem. Phys.* **108** 7747
- [16] Caillol J M, Levesque D and Weis J J 1997 *J. Chem. Phys.* **107** 1565
- [17] Orkoulas G and Panagiotopoulos A Z 1999 *J. Chem. Phys.* **110** 1581
- [18] See e.g. Plischke M and Bergersen B 1989 *Equilibrium Statistical Physics* (Englewood Cliffs, NJ: Prentice-Hall)
- [19] Leote de Carvalho R J F and Evans R 1995 *J. Phys.: Condens. Matter* **7** L575
- [20] Lee B P and Fisher M E 1996 *Phys. Rev. Lett.* **76** 2906
Fisher M E and Lee B P 1996 *Phys. Rev. Lett.* **77** 3561
- [21] Bekiranov S and Fisher M E 1999 *Phys. Rev. E* **59** 492
- [22] Schröer W and Weiss V C 1998 *J. Chem. Phys.* **109** 8504
Schröer W and Weiss V C 1999 *J. Chem. Phys.* **110** 4687
- [23] Weiss V C and Schröer W 1998 *J. Phys.: Condens. Matter* **10** L705
- [24] McCoy B F and Davis H T 1979 *Phys. Rev. A* **20** 1201
- [25] Groh B, Evans R and Dietrich S 1998 *Phys. Rev. E* **57** 6944
- [26] Evans R 1979 *Adv. Phys.* **28** 143
- [27] Rowlinson J S and Widom B 1982 *Molecular Theory of Capillarity* (Oxford: Clarendon)

- [28] See e.g. Hansen J-P and McDonald I R 1986 *Theory of Simple Liquids* (London: Academic)
- [29] Schröder W and Weiss V C 1997 *J. Chem. Phys.* **106** 7458
- [30] Davis H T 1995 *Statistical Mechanics of Phases, Interfaces and Thin Films* (New York: VCH) and references therein
- [31] Cahn J W and Hilliard J E 1958 *J. Chem. Phys.* **28** 258
- [32] Telo da Gama M M, Evans R and Sluckin T J 1980 *Mol. Phys.* **41** 1355
- [33] Smit B, Esselink E and Frenkel D 1996 *Mol. Phys.* **87** 159
- [34] Ennis J, Kjellander R and Mitchell D J 1995 *J. Chem. Phys.* **102** 975
- [35] Leote de Carvalho R J F and Evans R 1994 *Mol. Phys.* **83** 619
- [36] Heyes D M and Clarke J H R 1979 *J. Chem. Soc., Faraday Trans. II* **75** 1240